2021 IEEE 17th International Conference on Automation Science and Engineering (CASE)
August 23-27, 2021. Lyon, France

Optimized Static Gait for Quadruped Robots Walking on Stairs*

Linqi Ye, Yaqi Wang, Xueqian Wang*, Houde Liu and Bin Liang

2021 IEEE 17th International Conference on Automation Science and Engineering (CASE) | 978-1-6654-1873-7/21/$31.00 ©2021 IEEE | DOI: 10.1109/CASE49439.2021.9551433

***Abstract*—An optimized static gait that combines pose optimization, motion sequence optimization, and a novel high-level planning algorithm is proposed for quadruped robots to walk on stairs. Firstly, an optimized pose is determined for the robot to stand on stairs statically. Then, a climbing gait cycle with an optimized motion sequence is presented, which takes the robot from one position and pose to another position and pose. Finally, a high-level planning algorithm is proposed to adjust the step length in each gait cycle to enable the robot to safely walk along the stairs. The proposed static gait maximizes the stair-climbing capability significantly while still guaranteeing walking safety, which provides a general solution for quadruped robots to walk on stairs of different sizes. Several simulations in V-REP are presented to evaluate the effectiveness of the optimized static gait generation technique in improving the stair-climbing capability. Compared to other quadruped robots developed recently, the robot tested in this paper can walk on a regular staircase with a rise of 20 cm and an inclination of 37.6°, and can also climb over a few steep narrow steps with a rise of 18 cm and a run of 5 cm.**

I. Introduction

Compared to wheeled or tracked robots, quadruped robots have discrete contact points with the ground which makes them more capable of transversing rough terrain. Recently, more and more research groups including Boston Dynamics, MIT, and ETH are making great efforts to develop useful quadruped robots. Their products Spot, ANYmal, and MIT Cheetah represent the state of the art in this field. In the near future, quadruped robots are promising to help people in various aspects, such as field prospection, relief and rescue, industrial inspection, just to name a few.

Gait planning is the essential part for quadruped robots to transverse rough terrains. Inspired by the four-legged animals in the natural world, especially dogs and horses, a variety of gaits have been presented for quadruped robots. During quadruped walking, some legs keep contact with the ground to support the body, while the other legs swing in the air. According to the scheduling of the supporting leg and swing leg (namely, the walking pattern), quadruped gaits can be divided into walk, trot, pace, bound, gallop, etc. Among them, the walk gait is also called static gait, where at least three legs are in contact with the ground at any time. The convex hull of the contact feet forms the support polygon, and the projection of the center of mass (CoM) always stays within the support polygon during static walking. The other gaits belong to dynamic gaits, where the support polygon is very narrow so that the robot cannot keep statically balanced and has to step frequently to achieve dynamic stability.

The ability to climb stairs is one critical skill for quadruped robots to operate in real life. Several quadruped robots have shown successful trials in stair climbing during the last decades. Static gait was used earlier since it has a wide stability margin and is easy to implement. The TITAN series robots built in Tokyo Institute of Technology were pioneers, where TITAN III [1] can autonomously walk over stairs using the "whisker sensor" and TITAN VI [2] can climb ordinary stairs of 30-40^o by using an articulated body. In [3], a static stair-climbing gait was developed for a hybrid quadruped robot built by Harbin Institute of Technology. In [4], a gait based on central pattern generator (CPG) with online parameter tuning was applied to a puppy robot called AIBO and achieved adaptive walking on a small staircase. In [5], a static gait with optimized swing leg trajectory was proposed for a quadruped robot named Pegasus in Chinese University of Hong Kong, which allows it to cross stairs automatically. In [6], a novel pose optimization approach was presented for the ANYmal robot, which enables it to climb over significant obstacles, including a standardized set of stairs with a rise of 17 cm and a run of 29 cm. Compared to static gait, dynamic gait can reach high walking speed and recover from disturbances through fast foot placement. During the "Learning Locomotion" program launched by DARPA in 2005, research teams from Stanford University [7] and Institute for Human and Machine Cognition [8] designed a special dynamic jumping gait for the LittleDog robot, which achieved amazing performance to climb over steps nearly as tall as the robot's leg. Similarly, in [9], the Minitaur quadruped robot, which uses a parallel-elastic leg mechanism, can bound up stairs with 19.6cm height just like a frog. Recently, the trot gait has been applied to several versatile quadruped robots, including Spot [10], MIT Cheetah [11], and SCalf [12], all showing success for the stair-climbing tasks. Among them, Spot has shown very impressive performance in climbing stairs with autonomous navigation, while MIT Cheetah is able to blindly climb stairs covered in debris through model predictive control and a contact detection algorithm.

To sum up, both static and dynamic gaits have been investigated for stair climbing of quadruped robots, and some of them have shown the capability to walk on standard-sized stairs. In our opinion, although dynamic gait facilitates walking speed, it is less efficient in load capacity and safety compared to static gait, especially when walking on stairs, where dynamic gait is more likely to fail, which may cause severe damage to the robot. Therefore, it is worthy of studying how to walk safely and simultaneously maximize the stair-climbing capability by using static gait. To this end, an

*This work was supported by National Natural Science Foundation of China (62003188, 61803221, and U1813216), Guangdong Special Branch Plan for Young Talent with Scientific and Technological Innovation (2019TQ05Z111).

L. Ye, Y. Wang, X. Wang, and H. Liu are with the Center for Artificial Intelligence and Robotics, Tsinghua Shenzhen International Graduate School, Tsinghua University, 518055 Shenzhen, China (e-mail: {ye.linqi, wang.xq, liu,hd}@sz.tsinghua.edu.cn, yq-wang19@mails.tsinghua.edu.cn).

B. Liang is with the Navigation and Control Research Center, Department of Automation, Tsinghua University, 100084 Beijing, China (e-mail: bliang@tsinghua.edu.cn).

optimized static gait is proposed for a quadruped robot named THU-QUAD II in this paper. Focused on the walking safety and capability, several factors have been taken into account, such as kinematic constraints and collision avoidance, and both body pose optimization and motion sequence optimization have been conducted on the robot. Moreover, a novel high-level planning algorithm is proposed to generate footholds along the stairs automatically. The proposed methods have been tested on a quadruped robot named THU-QUAD II in the V-REP simulation environment. The simulation results show that the robot can climb stairs with a rise of 20 cm and an inclination of 37.6°， which demonstrates the improvement in the stair-climbing capability compared to other quadruped robots as shown in Table I. Besides, the proposed algorithm also allows the robot to climb over a few steep narrow steps with a rise of 18 cm and a run of 5 cm, which is difficult to achieve by other quadruped robots.

TABLE I.

STAIR-CLIMBING CAPABILITIES OF SEVERAL QUADRUPED ROBOTS

Robot	Year	Leg length	Gait Type	Stair Parameter (rise/run, inclination)
LittleDog[7-8]	2011	13cm	jump	12/28cm (23°)
Minitaur[9]	2017	28cm	bound	19.6/27.9cm (35°)
Spot[10]	2018	84cm	trot	17.8/27.9cm (33°)
MIT Cheetah[11]	2018	68cm	trot	17.8/27.9cm (33°)
ANYmal[6]	2018	50cm	static	17/29cm (30°)
Pegasus [5]	2019	75cm	static	8/30cm (15°)
THU-QUAD II	2020	60cm	static	20/26cm (37.6°)

The remainder of this paper is organized as follows. In Section II, the prototype quadruped robot THU-QUAD II is introduced. Then, pose optimization is discussed in Section III and motion sequence optimization is presented in Section IV. A high-level planning algorithm is developed in Section V. Finally, simulation results are given in Section VI and conclusions are summarized in Section VII.

II. PROTOTYPE QUADRUPED ROBOT

The prototype quadruped robot, THU-QUAD II, is shown in Fig. 1. This robot adopts the classical roll-pitch-pitch structure for each leg and uses 12 Kollmorgen's RGM20 robotic joint modules in total. The upper and lower links of each leg have an equal length of 30cm. Other specifications of THU-QUAD II are shown in Table II. The design of THU-QUAD II has paid special attention to achieving a wide range of motion for the joints, which allows it to switch between different configurations. By changing the bending direction of the legs, this robot is able to transform into any of the four commonly used leg configurations for quadruped robots, i.e., the backward/backward configuration, the forward/forward configuration, the forward/backward configuration, and the backward/forward configuration [13].

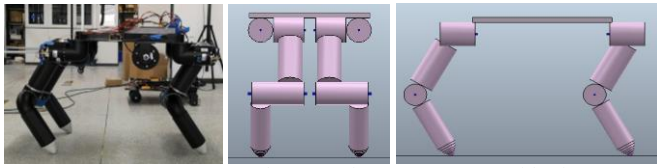

(a) THU-QUAD II (b) Front view (c) Side view

Figure 1. THU-QUAD II and its V-REP model views.

TABLE II.

SPECIFICATIONS OF THU-QUAD II

Size (L × W × H, fully stretched legs)	0.72m×0.4m×0.6m
Weight	45kg (about 8 kg for each leg)
Degrees of Freedom	12 (3 per leg)
Range of Motion	Hip abduction adduction (HAA): 270°, Hip flexion extension (HFE): 330°, Knee flexion extension (KFE): 330°
Joint Speed	15rpm
Joint Torque	61Nm

III. POSE OPTIMIZATION

To simplify the design process, the stair climbing task can be decomposed into two problems. The first problem is to figure out a series of static poses for the quadruped robot when it locates on different positions along the stairs. And the second problem is to design a set of motion sequences to take the robot from one position and the corresponding pose to the next position and its related pose under static stability. For overall consideration of safety and capability, optimization will be taken in both problems. In this section, we will focus on the body pose optimization.

When a quadruped robot is standing on stairs, the body of the robot becomes a mobile platform with six degrees of freedom. The pose of the body will significantly affect the robot in many aspects, such as kinematic reachability, torque distribution, and so on. Unlike walking on level ground, the height difference between the front and hind feet are frequently changing as the robot moves along a staircase. Therefore, it is important to adjust the body pose in the procedure to let the robot be more adapted to the stairs. For simplicity, we only consider the case when the robot has no roll, yaw, or sideway movement so that the pose can be treated in 2D. The two front legs and the two hind legs are overlapped, as seen from the side face. Under those conditions, some possible poses of a quadruped robot standing on stairs are shown in Fig. 2. Generally, the pose can be quantified by three kinds of parameters: 1) the leg bending direction, 2) the CoM position, and 3) the body pitch angle.

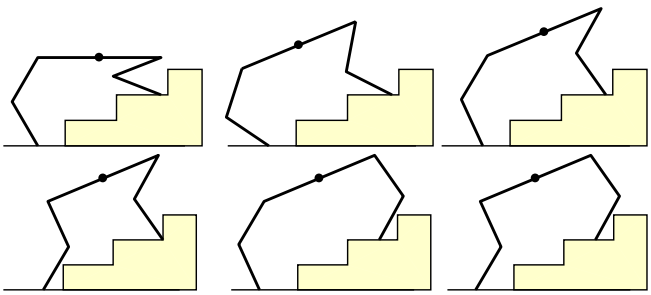

Figure 2. Possible poses for a quadruped robot standing on stairs.

(1) Leg bending direction

Each leg of the robot has three degrees of freedom. When a nonsingular position is given for a foot relative to the body, there are always two solutions for the joint angles. To avoid collision with the stairs, the robot should bend its legs to the downstairs direction, especially when walking on narrow stairs. Therefore, the three poses at the bottom of Fig. 2 are not preferred.

(2) CoM position

To achieve maximum stability margin, the projection of the CoM should be placed in the middle of the support rectangle formed by the four feet. In the top middle of Fig. 2, the CoM projection is closer to the feet on the lower side, which means the robot is more likely to fall to the lower feet side.

Based on the above analysis, we put forward the following two basic requirements: 1) all legs bend to the downstairs direction; 2) the projection of the CoM locates in the middle between the front and rear legs. After excluding the poses that violate the above requirements, there are still many available options because of the differences in the body pitch angle, which is analyzed in the following.

(3) Body pitch angle

Due to the height difference between the front and rear feet, the body pitch angle will significantly influence the available workspace of each foot. Intuitively, we choose three typical poses as candidates. Figs. 3-5 show the candidate poses under different step heights. The first denoted as "Candidate A" is shown in Fig. 3, where the body keeps level with constant height and the foot places under the hip. The second denoted as "Candidate B" is shown in Fig. 4, where the body pitches to keep parallel with the virtual slope formed by the front and rear feet and the foot places under the hip. The third denoted as "Candidate C" is shown in Fig. 5, where the body pitches to keep parallel with the virtual slope formed by the front and rear feet and the horizontal distance between the front and rear feet keeps constant.

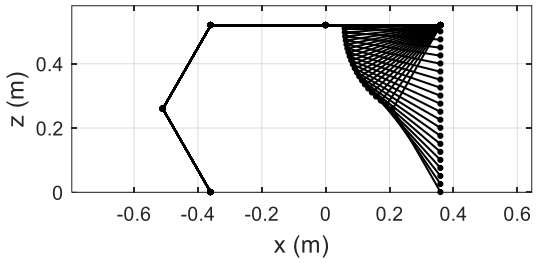

Figure 3. Pose Candidate A. *The body keeps level with constant height and the foot places under the hip.*

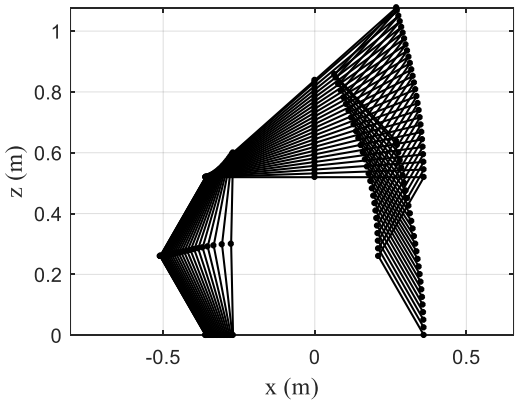

Figure 4. Pose Candidate B. *The body pitches to keep parallel with the virtual slope formed by the front and rear feet. The foot places under the hip. As a result, the horizontal distance between the front and rear feet decreases for a higher step height.*

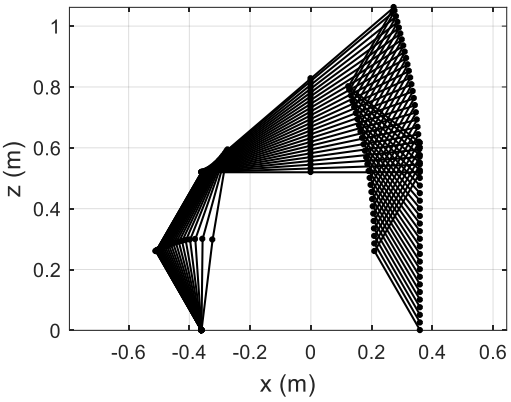

Figure 5. Pose Candidate C. *The body pitches to keep parallel with the virtual slope formed by the front and rear feet. The horizontal distance between the front and rear feet keeps constant for different step heights.*

To figure out the best pose, three selected indexes are analyzed for the three pose candidates in the following.

(1) Maximum step height

For Candidate A, as can be seen from Fig. 3, the maximum step height is limited by the body height. For Candidate B and C, as observed from Fig. 4 and Fig. 5, the step height reaches the maximum when the legs on the lower side become straight. Specifically, the maximum step heights for the three candidates are numerically computed as A: 0.52m, B: 0.64m, and C: 0.62m. Therefore, the maximum step height of Candidate B slightly exceeds Candidate C and is much higher than Candidate A.

(2) Knee torque

The knee torques for the three pose candidates are different. Fig. 6 shows three candidate poses with the same step height. As can be observed, for Candidate A, the legs on the upper side bend much more than the legs on the lower side. Therefore, the knee joint on the upper-side legs has a longer moment arm, which produces a bigger torque. While for Candidate B and C, all legs bend nearly the same, so the knee torques are evenly distributed to all legs. And the moment arm for the knee joint in B and C is shorter than that in the upper-side leg of A, which leads to smaller knee torque.

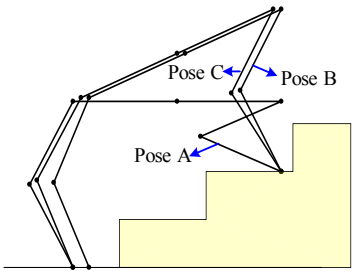

Figure 6. Three candidate poses with the same step height.

(3) Complexity

Among the three candidates, Candidate A is the simplest, which does not require for pitch. For Candidate B, the horizontal distance between the front and rear feet changes for different step heights, which makes it more difficult to implement than Candidate C.

According to the above analysis, a comprehensive comparison between the three pose candidates is summarized in Table III. As can be seen, Candidate B and C can reach a higher step height than A and use less knee torque than A, which verifies the advantage of using body pitch when walking on stairs. Between B and C, they exhibit very close performance but C is simpler than B since it uses the constant horizontal distance between the front and rear feet, which is easier to implement. Therefore, after making trade-offs between the three indexes, we finally choose Candidate C as the optimized pose.

TABLE III.

COMPARISON BETWEEN THE POSE CANDIDATES

Maximum step height (bigger is better)	B≈C>A
Knee torque (smaller is better)	B≈C<A
Complexity (smaller is better)	A<C< B

Formally, we describe the optimized pose as follows. As shown in Fig. 7, let h be the step height between the front and hind feet, H and L be the normal body height and front-rear foot distance on level ground, respectively. Then the optimized pose on stairs can be described by four rules as follows.

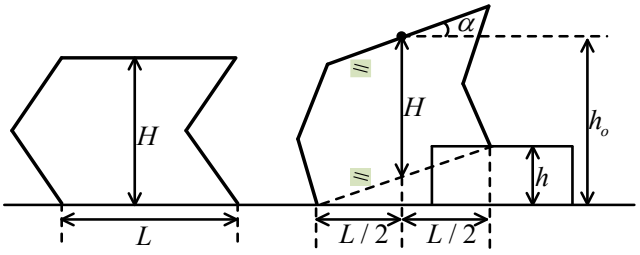

Figure 7. The optimized pose on stairs.

Rule 1 (Leg bending direction): All legs bend to the downstairs direction.

Rule 2 (Pitch angle): The body keeps parallel with the "virtual slope" formed by the front and the hind feet. Denote the pitch angle of the body as α, then it follows that

$$\alpha = \arctan(h / L). \tag{1}$$

Rule 3 (Body Height): The body height equals a constant height plus the average height of the front and hind feet. Denote the height of the body as h_o. Then we have

$$h_o = H + h / 2. \tag{2}$$

Rule 4 (Foot position): The horizontal distance between the front feet and hind feet keeps constant, while the projection of the COM lies in the middle.

The above rules have built a one-to-one mapping between the step height and the body pose. Once the step height is given, the pose of the robot can then be fully determined. This completes the pose optimization part.

IV. MOTION SEQUENCE OPTIMIZATION

After determining the optimal pose for the robot, the next step is to let the robot move along the stairs. Based on the modular idea, we only need to figure out how to let the robot transform from one position and pose to the next position and pose. This transformation forms a climbing gait cycle.

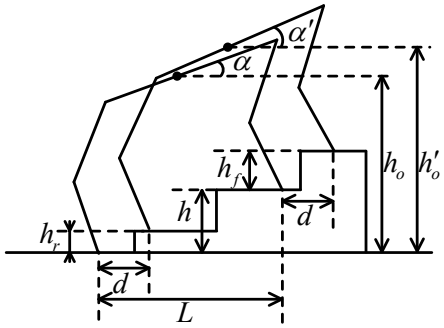

Figure 8. Diagram of a climbing gait cycle.

Fig. 8 shows a representative case of a climbing gait cycle, where the front feet change the height of h_f and the rear feet change h_r. Denote h as the initial height difference between the front and rear feet and d as the walking distance. Then a climbing gait cycle can be fully described by four parameters (h, h_f, h_r, d).

Denote the pitch angles of the body at the beginning and the end of the gait cycle as α, α', respectively. It follows that

$$\begin{aligned} \alpha &= \arctan(h / L), \\ \alpha' &= \arctan\left[(h + h_f - h_r) / L\right], \end{aligned} \tag{3}$$

according to Rule 2. This indicates the robot should pitch its body with the angle of $\Delta\alpha = \alpha' - \alpha$ during one gait cycle.

Denote the heights of the body at the beginning and the end of the gait cycle as h_o, h'_o, respectively. Then we have

$$\begin{aligned} h_o &= H + h / 2, \\ h'_o &= H + (h + h_f + h_r) / 2, \end{aligned} \tag{4}$$

according to Rule 3. Therefore, the robot should raise its body for the height of $\Delta h_o = h'_o - h_o$ during one gait cycle.

To maintain static stability during a gait cycle, a set of motion sequences need to be carefully specified. In [13], we have developed a motion sequence for static walking on level ground as shown in Fig. 9, where the robot executes body shift and leg swing alternately to keep static balance. Similarly, we can design the stair-climbing motion sequence by adding additional adjustment of the body height and pitch angle.

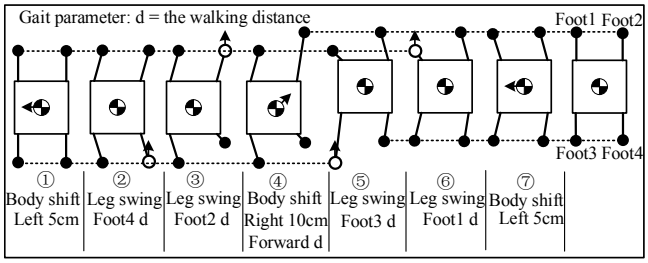

Figure 9. The motion sequence for static walking on level ground.

The motion sequence of a climbing gait cycle is more complicated. To show the motion sequence clearly, we

develop a gait cycle diagram. As an illustration, the motion sequence in Fig. 9 can be transformed into a gait cycle diagram as depicted in Fig. 10. In the gait cycle diagram, the body and four feet of the quadruped robot are represented by four little circles. We use green to represent body movement and orange to represent leg swing. And the inserted codes indicate the movement to execute, where "x", "y", and "z" represent movements in the three axes, respectively. In addition, the single-row codes execute simultaneously while the multi-row codes execute sequentially. This allows us to describe complicated motion sequences.

Now consider the motion sequence for a climbing gait cycle. Since climbing up and down stairs are inverse processes, they have totally reversed motion sequences. Therefore, we only need to consider one of them. Here we focus on the climbing-up walking.

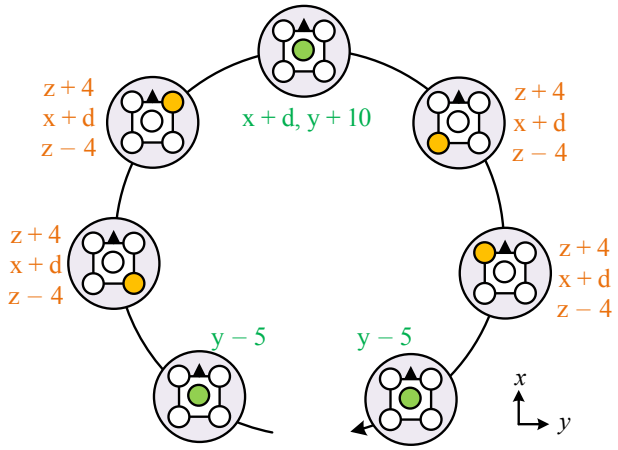

Figure 10. Gait cycle diagram for static walking on level ground. *Green represents body movement and orange represents leg swing. The single-row codes execute simultaneously while the multi-row codes execute sequentially.*

When adding body pitch to the motion sequence, there are several choices by inserting the pitch motion into different positions in the sequence. Two typical choices are doing pitching before or after the front feet climbing on the stair, which are analyzed as follows.

(1) Pitch before climb

In this situation, the robot adjusts the body pitch angle for $\Delta\alpha$ before the front legs proceed to climb stairs. However, as shown in Fig. 11, the front feet may leave the ground for a big $\Delta\alpha$ when climbing a high step.

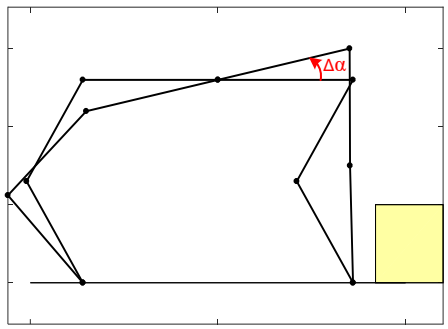

Figure 11. Pitch before climb may cause foot off ground.

(2) Pitch after climb

In this situation, the robot adjusts the body pitch angle for $\Delta\alpha$ after both front legs have climbed on the step. However, as shown in Fig. 12, it may cause an unreachable foot trajectory for the second front foot if the step height h_f is too high. In Fig. 12, the green area shows the reachable space of the front feet. Due to the HFE angle limit in our robot, a half circle under the body is unreachable since the upper link of the leg cannot pass through the body. During the first front leg swing phase, the swing foot is a little ahead of the hip, and thus the reachable step height is relatively high. But during the second front leg swing phase, the body has moved forward, and the swing foot is behind the hip, which results in a reduced step height. This is why it may cause an unreachable foot trajectory by doing pitch after climb.

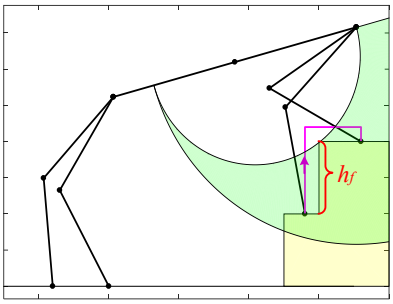

Figure 12. Pitch after climb may cause an unreachable foot trajectory. *The green area shows the reachable space of the front feet.*

After analyzing the two choices above, it can be concluded that both of them have some drawbacks. To overcome the discovered problems, we propose an optimized motion sequence as shown in Fig. 13. The key relies on a particularly-designed compound motion as marked by red in the figure, where the body pitch motion (represented by "p" in the code) is taken at the same time when the second front leg is lifting up, and the body height raises together with the pitch motion. In this way, the front hip rises together with the front foot, which allows the front foot to reach a much bigger step height.

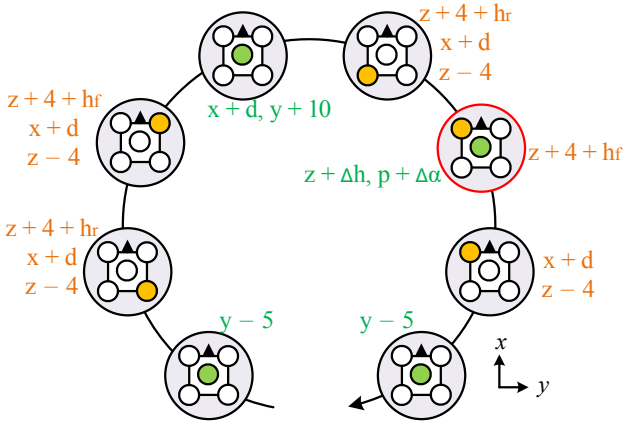

Figure 13. Gait cycle diagram for static walking on stairs.

It should be noted that the motion sequence in Fig. 13 is designed for walking upstairs. When the robot is walking downstairs, the corresponding motion sequence should be reversed.

V. HIGH-LEVEL PLANNING

Based on the optimized climbing gait cycle developed in the previous section, now we can proceed to do high-level planning to ensure the robot crosses the stairs safely. The basic idea is to adjust the gait parameters (h, h_f, h_r, d) for each gait cycle in real time according to the position of the robot on the stairs.

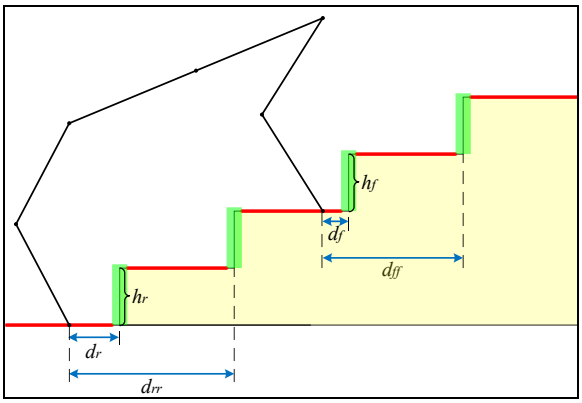

Figure 14. Gait planning for stair climbing. *To ensure safety, the robot should put its foot on the red line area and avoid the green area.*

Fig. 14 shows a quadruped robot on stairs. To guarantee walking safety, the foothold should keep away from the region close to the edge of the steps. Therefore, a safety distance of 2cm is selected around the step edge. To avoid collision or slide off, the robot should put the foot on the red line area while avoiding the green area. This can be achieved by selecting an appropriate walking distance d.

In Fig. 14, d_f, d_{ff}, d_r, d_{rr} are distances from the front and rear feet to the step edges, and h_f, h_r are the height of the steps. Considering the kinematic constraints, we choose a maximum step length of 15cm for each gait cycle. Therefore, we can determine whether a foot can climb onto the next step according to its distance from the step edge. For example, for the front foot, if $d_f < 15-2 = 13$cm (2 represents the value of the safety distance), then it can step onto the next step. Otherwise, it should stay on the same step. Therefore, according to the values of d_f, d_{ff}, d_r, d_{rr}, there are four situations in total to be considered, as shown in Table IV. In the four situations, the robot takes an action of "full climb", "rear climb", "front climb", or "no climb", respectively, and the corresponding gait parameters are given.

TABLE IV.

GAIT PARAMETERS IN DIFFERENT SITUATIONS

	$d_f \le 13$cm	$d_f > 13$cm
$d_r \le 13$cm	**Full climb:** 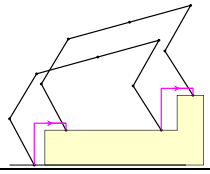 $\Delta h_f = h_f, \Delta h_r = h_r$ $d = \min\{15, d_{ff}-2, d_{rr}-2\}$	**Rear climb:** 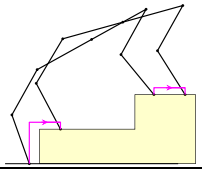 $\Delta h_f = 0, \Delta h_r = h_r$ $d = \min\{15, d_f-2, d_{rr}-2\}$
$d_r > 13$cm	**Front climb:** 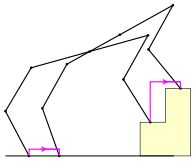 $\Delta h_f = h_f, \Delta h_r = 0$ $d = \min\{15, d_{ff}-2, d_r-2\}$	**No climb:** 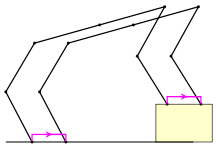 $\Delta h_f = 0, \Delta h_r = 0$ $d = \min\{15, d_f-2, d_r-2\}$

With the parameters given in Table IV, the overall high-level planning algorithm for stair climbing is given in Fig. 15.

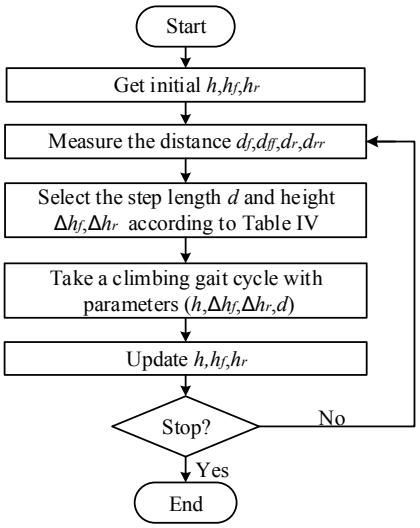

Figure 15. The high-level planning algorithm for stair climbing.

VI. SIMULATIONS

To demonstrate the effectiveness of the proposed method, simulations are performed in the V-REP software with the Newton physics engine. Two kinds of stairs with different sizes are considered.

Scenario 1: A regular staircase with high inclination

The first scenario is shown in Fig. 16, where a symmetric staircase with 10 steps is built. The staircase has a rise of 20 cm and a run of 26 cm, which means the inclination is 37.6°, steeper than the test scenarios in other quadruped robots as previously listed in Table I.

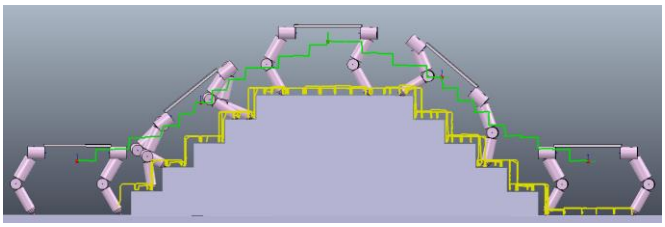

Figure 16. Simulation results for Scenario 1.

By using the proposed static gait, the robot finally crosses the entire staircase successfully. Several snapshots of the robot are recorded throughout the task, as shown in Fig. 16. The

green line represents the CoM trajectory, and the yellow line the foot trajectory. It can be seen that the body pose of the robot changes and adapts well with the stairs when in different positions. The robot first goes upstairs with a backward/backward configuration. After arriving at the top platform, it transfers the configuration from backward/backward to forward/forward to go downstairs. This reflects the requirement in Rule 1 for the optimized body pose proposed in Section III. In this way, the robot can effectively avoid collision with the stairs.

Scenario 2: A short staircase with narrow steps

The second scenario is a short staircase with three narrow steps. The staircase has a rise of 18 cm and a run of 5 cm. Although the height of each step is lower than that in Scenario 1, the inclination increases to 74.5° due to the narrow steps, which makes it a very challenging task. By using the proposed method, the robot successfully accomplishes this task, as can be seen from the snapshots in Fig. 17.

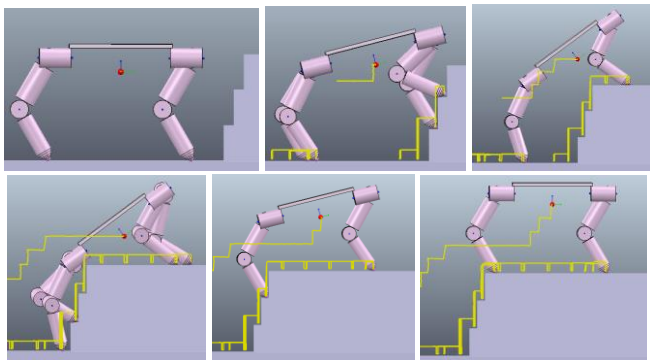

Figure 17. Simulation results for Scenario 2.

It should be noted that this task is almost impossible for the trotting gait. For quadruped robots with high torque density motors like MIT Cheetah, it may directly jump to the top stair. However, very few quadruped robots can have such amazing performance. Therefore, the proposed static gait has provided a more realistic way for general quadruped robots to cross such challenging obstacles.

Due to the lack of staircases with the given size, experiments only have been done for stairs with a rise of 15 cm and run of 30 cm and a doorsill with a height of 21 cm and a width of 28 cm, both succeeded. Other experiments will be taken in the future.

VII. Conclusion

An optimized static gait is proposed for a quadruped robot to walk on stairs by combining pose optimization, motion sequence optimization, and a high-level planning algorithm. The overall approach allows the quadruped robot to walk safely on stairs with maximized stair-climbing capability. The proposed method achieves better performance than some quadruped robots have shown recently, which are demonstrated through several simulations in the V-REP software.

However, the mechanical design of THU-QUAD II has not been optimized for stair climbing. One of the shortages comes from the HFE angle limit. As can be seen from Fig.1, the upper link of the leg cannot pass through the body, thus limiting the step height of the front leg, which is not good for stair climbing. This impact can be seen in the motion sequence optimization part in Section IV. We will try to improve the mechanical design in the future to avoid this problem.

References

[1] S. Hirose, Y. Fukuda, and H. Kikuchi, "The gait control system of a quadruped walking vehicle," *Advanced Robotics*, vol. 1, no. 4, pp. 289-323, 1986.

[2] S. Hirose, K. Yoneda, K. Arai, and T. Ibe, "Design of a quadruped walking vehicle for dynamic walking and stair climbing," *Advanced Robotics*, vol. 9, no. 2, pp. 107-124, 1994.

[3] B. Huang, L. Sun, and Y. Luo, "Statically balanced stair climbing gait research for a hybrid quadruped robot," in *IEEE International Conference Mechatronics and Automation*, vol. 4, pp. 2067-2071, 2005.

[4] C. Liu, Q. Chen, and D. Wang, "CPG-inspired workspace trajectory generation and adaptive locomotion control for quadruped robots," IEEE Transactions on Systems, Man, and Cybernetics, Part B (Cybernetics), vol. 41, no. 3, pp. 867-880, 2011.

[5] T. Liao, S. Ye, L. Chen, C. Sun, and A. Zhang, "Energy efficient swing leg trajectory planning for quadruped robots walking on rough terrain," in *IEEE International Conference on Robotics and Biomimetics (ROBIO)*, pp. 2128-2133, 2019.

[6] P. Fankhauser, M. Bjelonic, C. D. Bellicoso, T. Miki, and M. Hutter, "Robust rough-terrain locomotion with a quadrupedal robot," in *IEEE International Conference on Robotics and Automation (ICRA)*, pp. 1-8, 2018.

[7] J. Zico Kolter and A. Y. Ng, "The stanford littledog: A learning and rapid replanning approach to quadruped locomotion," *The International Journal of Robotics Research*, vol. 30, no. 2, pp. 150-174, 2011.

[8] P. D. Neuhaus, J. E. Pratt, and M. J. Johnson, "Comprehensive summary of the Institute for Human and Machine Cognition's experience with LittleDog," *The International Journal of Robotics Research*, vol. 30, no. 2, pp. 216-235, 2011.

[9] T. T. Topping, G. Kenneally, and D. E. Koditschek, "Quasi-static and dynamic mismatch for door opening and stair climbing with a legged robot," in *IEEE International Conference on Robotics and Automation (ICRA)*, pp. 1080-1087, 2017.

[10] https://www.youtube.com/watch?v=Ve9kWX_KXus

[11] J. Di Carlo, P. M. Wensing, B. Katz, G. Bledt, and S. Kim, "Dynamic locomotion in the mit cheetah 3 through convex model-predictive control," in *IEEE/RSJ International Conference on Intelligent Robots and Systems (IROS)*, pp. 1-9, 2018.

[12] G. Zhang, X. Rong, C. Hui, Y. Li, and B. Li, "Torso motion control and toe trajectory generation of a trotting quadruped robot based on virtual model control," *Advanced Robotics*, vol. 30, no. 4, pp. 284-297, 2016.

[13] C. Semini, *HyQ-design and development of a hydraulically actuated quadruped robot*. PhD thesis, University of Genoa, Italy, 2010.

[14] L. Ye, H. Liu, X. Wang, B. Yuan, and B. Liang, "Task-oriented hierarchical control for a quadruped robot," in IEEE International Conference on Robotics and Biomimetics (ROBIO), pp. 2146-2151, 2019.